

Article

Optimization and Field Test of a Chelating Acid System for Scaled Gas Wells in the Hechuan Gas Field

Qiang Li ^{1,2}, Zhenzhong Fan ^{1,*}, Qingwang Liu ^{1,*}, Guohong Liu ², Wenhai Ma ², Junliang Li ², Nan Li ² and Pingang Ma ²

¹ Petroleum Engineering College, Northeast Petroleum University, Daqing 163318, China; johnlee2013@126.com

² Daqing Oilfield Production Engineering Research Institute, Daqing 163453, China; liuguohong@petrochina.com.cn (G.L.); mawenhai@petrochina.com.cn (W.M.); lijunliang@petrochina.com.cn (J.L.); linanlinan@petrochina.com.cn (N.L.); mapingang@petrochina.com.cn (P.M.)

* Correspondence: fanzhenzhong@163.com (Z.F.); liuqingwang@163.com (Q.L.)

Abstract: The Hechuan gas field is one of the tight gas reservoirs with the highest formation water salinity in China. The content of metal ions, such as calcium, magnesium, iron, and barium, is as high as 20 g/L. Severe scales in near-wellbore reservoir blocks the gas and liquid flow paths, affecting the normal production of gas wells. The analysis of scale samples shows that the scale compositions in the Hechuan gas field are complex, which are composed of calcium carbonate, calcium sulfate, barium sulfate, iron salt, silicate, and other inorganic scales. To dissolve these scales, 14 kinds of laboratory self-made chelating acids named AST-01 to AST-14, sequentially, were evaluated by the descaling rate, in which the chelating acid AST-01 was selected with a dissolution rate of 77.7%. Meanwhile, the optimal concentration and reaction time of AST-01 were investigated, and the concentrations of the corrosion inhibitor, the iron ion stabilizer, and surfactants were also optimized. Then, a chelating acid descaling formula was obtained, which was 15~20% of AST-01 chelating acid + 1.5~2.0% of corrosion inhibitor + 2.5% of iron ion stabilizer + 0.3% of drainage aid. A pilot field trial of this descaling formula was applied in a Hechuan X1 well. A remarkable result was obtained in that the shut-in tubing pressure recovery rate was increased by 14 times, the gas production was increased by 10 times, and the gas well resumed to produce continuously again.



Citation: Li, Q.; Fan, Z.; Liu, Q.; Liu, G.; Ma, W.; Li, J.; Li, N.; Ma, P. Optimization and Field Test of a Chelating Acid System for Scaled Gas Wells in the Hechuan Gas Field. *Energies* **2021**, *14*, 7959. <https://doi.org/10.3390/en14237959>

Academic Editors: Kun Sang Lee and Riyaz Kharrat

Received: 20 October 2021

Accepted: 18 November 2021

Published: 29 November 2021

Publisher's Note: MDPI stays neutral with regard to jurisdictional claims in published maps and institutional affiliations.



Copyright: © 2021 by the authors. Licensee MDPI, Basel, Switzerland. This article is an open access article distributed under the terms and conditions of the Creative Commons Attribution (CC BY) license (<https://creativecommons.org/licenses/by/4.0/>).

Keywords: Hechuan gas field; carbonate and sulfate scales; chelating acid; descaling; high salinity

1. Introduction

The Hechuan Gas Field is located in the central part of the Sichuan Basin. The main development stratum is the Xujiache formation, and the reservoir permeability is generally less than 0.05 mD, which belongs to tight sandstone reservoirs [1]. Almost all gas wells in the Hechuan gas field produce high salinity formation water, which is on average 183 g/L [2]. The main cations and anions of formation water are K^+ , Na^+ , Ca^{2+} , Mg^{2+} , Ba^{2+} , Fe^{2+} , Fe^{3+} , Al^{3+} , and Zn^{2+} , and S^{2-} , Cl^- , SO_4^{2-} , and CO_3^{2-} . The total content of calcium, magnesium, barium, iron, and other metal ions is more than 20 g/L, which provides a sufficient source for gas well scaling [3]. Meanwhile, due to the changes in temperature and pressure conditions when gas and water flow through perforation borehole, downhole choke valves, gas nozzles, and other downhole tools, the scales are prone to settle and become thicker and thicker around these flow channels [4–6].

Once scaling begins, the production of gas wells will go through three stages: the decline of wellhead pressure and production, intermittent production, and well shut-in. In 2020, it was found that the 28 downhole chokes were seriously blocked after being fished out from 35 low-pressure gas wells in the Hechuan gas field. Scaling of gas wells further leads to lower production of gas wells in this tight sandstone gas reservoir. Therefore, there

is an urgent need to develop an efficient descaling method to ensure the normal production of gas wells.

At present, the descaling methods mainly include physical and chemical methods [7]. The physical descaling methods, such as mechanical drilling [8], waterjet [9–11], or ultrasonic [12,13] are useful in breaking down the scales. However, the application of these methods is limited by the size of the downhole tubing strings and the location of the downhole tools [14,15]. On the contrary, the chemical descaling methods [16] are applying chemical agents to dissolve solid scales [17–19] or using inhibitors to slow down the formation of scale [20–22] with a simpler process, a lower cost, and a short shut-in time compared to physical descaling methods [23].

In this study, the chemical descaling method was adopted. Firstly, the scale samples were analyzed by Energy Dispersive X-ray Spectroscopy (EDS) to speculate the scale compositions. The result showed that the scales contained calcium carbonate, calcium sulfate, barium sulfate, iron salts, etc. However, conventional acidic solutions [24,25] such as hydrochloric acid and mud acid (HF/HCl = 15 wt%/8 wt%) are not suitable as they cannot dissolve sulfate scales and may cause secondary precipitation. Through a literature review, it was found that the chelating group [26–30] in the chelating acid [31–34] could chelate with the metal ions to increase the dissolution rate of the sulfate scales, and the acid solution also had a significant effect on carbonate scales. Then, we tried 14 kinds of laboratory self-made chelating acids named AST-01 to AST-14 to show their descaling rate on Hechuan scale samples, in which chelating acid AST-01 was screened out as the main acid for the highest descaling rate. Meanwhile, the concentrations of corrosion inhibitor, iron ion stabilizer, and drainage aid were studied in this paper. At last, a field test was carried out in a scale plugging gas well and a good result was achieved.

2. Experimental Materials and Methods

2.1. Chemicals and Materials

Chemicals: Chelating acids AST01~AST14 (60 wt%), corrosion inhibitor (octadecyl trimethyl ammonium bromide 99 wt%), surfactants (fluorocarbon surfactants, nonionic hydrocarbon surfactants, and small molecular alcohols in a ratio of 1:60:15), and purified water were made in the laboratory. Absolute ethyl alcohol, kerosene, acetone, bentonite, cyclohexane, sodium carbonate, ammonium hydroxide, potassium chloride, and iron (III) chloride hexahydrate were all purchased from Chengdu Kelong Chemical Co., Ltd., Chengdu City, China. The sulfosalicylic acid indicator was from Dongguan Wanjiang Zhaolong Sign Business Department, Dongguan City, China.

Materials: The N80 sheet steel was obtained from the Motian Electronic Instrument Co., Ltd., Gaoyou City, China. PTFE tape was bought from Hangzhou Lin'an Gaina Fluoroplastic Co., Ltd., Hangzhou City, China. Six scale samples named sample (a) to sample (f) were collected from the Hechuan gas field.

2.2. Experimental Instruments

The SHA-C constant temperature water bath was from Changzhou Hengjiu Instrument Manufacturing Co., Ltd., Changzhou City, China. The TG16G centrifuge was from Changzhou Jintan Jingda Instrument Manufacturing Co., Ltd., Changzhou City, China. The DHG-9140A oven was from Shanghai Qixin Scientific Instrument Co., Ltd., Shanghai City, China. The MP-1002 analytical balance was from Ningbo Yong Hui Instrument Technology Co., Ltd., Ningbo City, China. The 10 mL pipette gun was from Jinan Oulaibo Electronic Commerce Co., Ltd., Jinan City, China. The 50 mL high temperature resistant large-caliber plastic bottle was from Zhejiang Yuhuan Xinhua Plastic Factory, Yuhuan County, China. The acid burettes, the volumetric flasks, etc. were all from Chengdu Kelong Chemical Co., Ltd., Chengdu City, China. X-ray energy spectrometer (X-Max50) was from Oxford Instruments, Abingdon, United Kingdom. The scanning electron microscope (Apreo2 C) from Thermo Fisher Scientific Co., Waltham, MA, USA.

2.3. Experimental Methods

2.3.1. Analysis of Scale Samples

A certain amount of each scale sample was weighted after drying and placed in a beaker, and then the cyclohexane was added with a solid–liquid ratio of 1:3. After being stirred thoroughly, the scale samples were centrifuged at 3000 r/min for 2 min to remove the oil components and dried in an oven at 80 °C to constant weight. Repeating the above steps 3 times, the average quality change of each scale sample was its oil content. The inorganic composition of the scale sample was estimated by energy spectrum analysis. The microscopic appearance of the scale sample was dried and sprayed with gold, then characterized by a scanning electron microscope.

2.3.2. Optimization Experiment of Chelating Acid

The performances of 14 chelating acids were evaluated based on their dissolution rate in the scale samples. The scale sample and a certain concentration of each chelating acid diluted with distilled water were filled into a 50 mL plastic centrifuge tube with the solid–liquid ratio of 1:20, labeled from AST-01 to AST-14, successively, and reacted for several hours in a water bath at 80 °C. Then, the samples were centrifuged at 5000 r/min for 5 min to separate liquid and solid phases, dried at 80 °C to constant weights. The residues were weighed to calculate the dissolution rate of each chelating acid according to the weight loss of the scale reaction.

2.3.3. Experimental Methods of Selecting Additive Concentrations

The concentration of the corrosion inhibitor optimized experiment was followed by the standard procedure of the People’s Republic of China Petroleum and Natural Gas Industry Standard SY/T 5404-2019 (performance test method and evaluation index of corrosion inhibitors for acidification). The corrosion inhibition rate was calculated as follows:

$$K = \frac{10^6 \Delta m_i}{A_i \Delta t} \quad (1)$$

$$E = 1 - \frac{K}{K'} \times 100\% \quad (2)$$

where K —corrosion rate of test piece with corrosion inhibitor, $g/(m^2 \cdot h)$; Δm_i —a weight loss of N80 sheet steel, g; A_i —the surface area of the N80 sheet steel, mm^2 ; Δt —experiment time, h; E —inhibition rate, %; and K' —corrosion rate of N80 sheet steel without corrosion inhibitor, $g/(m^2 \cdot h)$.

The optimal concentration of iron ion stabilizer experiment was conducted by China National Petroleum Corporation Enterprise Standard Q/SY TZ 0082-2015 (Technical requirements and test methods for iron ion stabilizers).

$$N = \rho_{Fe^{3+}} \frac{V_l}{V_s} \quad (3)$$

where N —the ability to stabilize iron ions, mg/mL; $\rho_{Fe^{3+}}$ —the content of iron ions in the iron standard solution, mg/mL; V_l —the volume and dosage of iron ion standard solution, mL; and V_s —the volume of iron ion stabilizer, mL.

3. Results and Discussion

3.1. Analysis of Scale Samples

The scale samples used in this experiment came from different locations of six gas wells, among which scale sample (a) was taken from the tubing depth of 2208–2210 m, scale sample (b) was retrieved from the downhole choke at depth of 1680 m, scale sample (c) was from the gas tree tubing hanger, scale sample (d) was from the outer wall of the tubing at 1205–1440 m, scale sample (e) was from the perforated well section at 2302–2315 m, and scale sample (f) was taken from the gas tree needle valve. The appearance and morphology

of dried samples are shown in Figure 1. Scale samples (a)~(f) are almost black in color, besides sample (e) with light yellow color. The dispersion of the six samples is also not the same. Sample (a), (d), and (e) have a good dispersibility, while samples (b), (c), and (f) are in the form of small clumps.

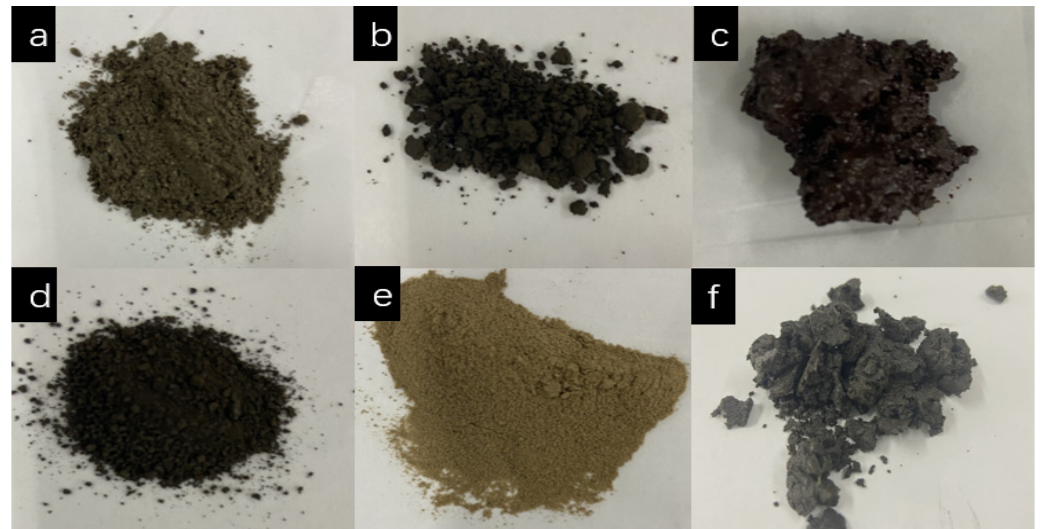


Figure 1. Morphology of scale samples from six gas wells.

The oil content analysis result of the six scale samples shown in Figure 2 is also quite different, in which the oil content in scale sample (c) is the highest, reaching 34.4%, and sample (f) reaches 23%, while the oil contents of the scale sample (a), (b), (d), and (e) are very low. The reason for the difference is that the scale samples were obtained from different well depths. As the scale samples (c) and (f) were obtained near the wellhead, the condensate oil precipitates from natural gas for the wellhead temperature and pressure are both lower than the dew point temperature and pressure, so the oil content is much higher.

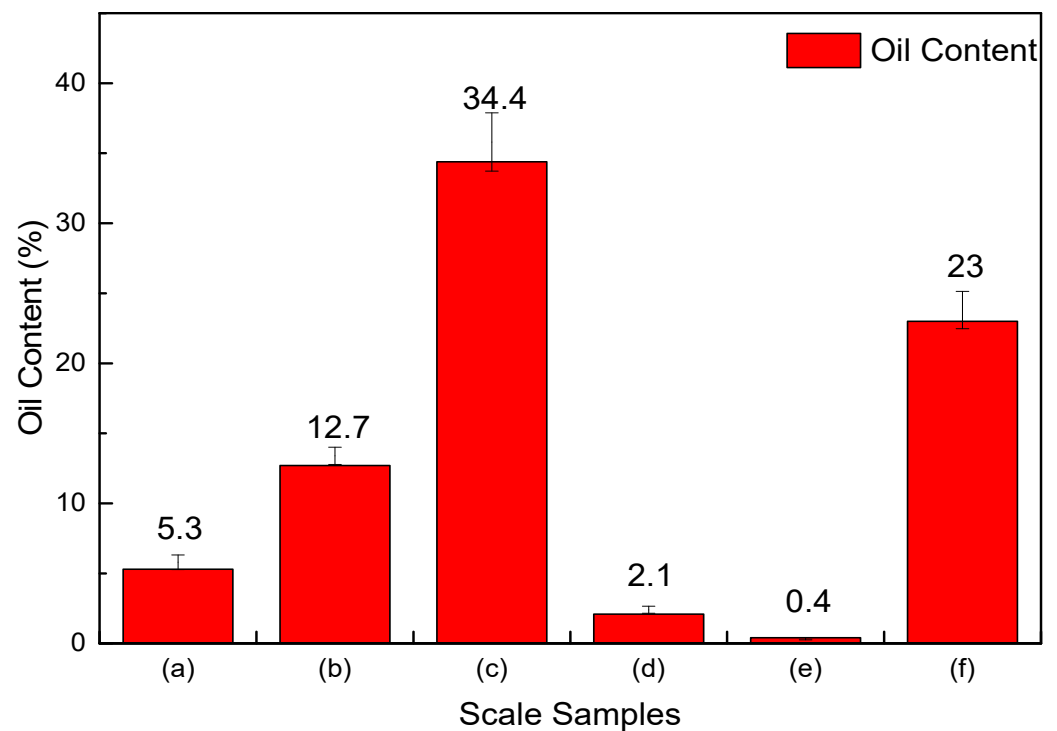


Figure 2. The average oil content of six scale samples.

The microscopic morphological analysis of scale samples by scanning electron microscopy is shown in Figure 3. It can be seen that the surfaces of the sample (c) and (f) are not smooth, and there are many small particles attached to their surfaces. This phenomenon can be explained when combined with oil content analysis. Due to their higher oil content, it makes the scale samples adhesive. The higher the oil content, the stronger the adhesion and the more uneven surface of scales.

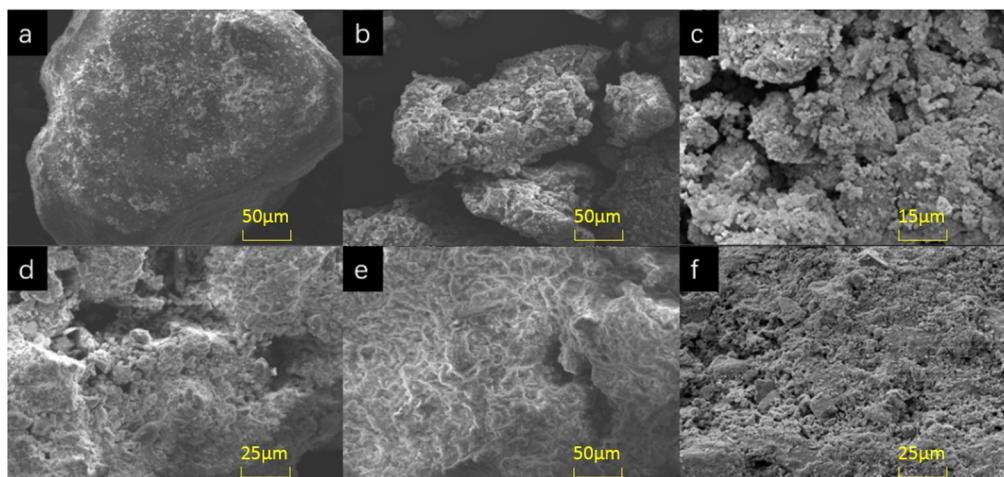


Figure 3. Microscopic morphology of scale samples ((a–f) represents scale sample (a) to sample (f), respectively).

In Figure 4, the inorganic composition analysis by dot scan EDS shows that the main elements of all the scale samples are basically the same. Elements C, O, Ca, Ba, Mg, Fe, and S are relatively higher in the six scale samples, followed by Si, Al, and other elements. According to the elements of each scale sample, the compositions can be inferred as calcium carbonate, calcium sulfate, barium sulfate, formation sands, and iron salts, etc. The main speculated composition of each scale sample is shown in Table 1.

Table 1. The speculated compositions of each scale.

Scale Sample	Components
(a)	CaCO ₃ , BaSO ₄ , CaSO ₄ , SiO ₂ , Al ₂ O ₃ , and Iron salts
(b)	CaCO ₃ , CaSO ₄ , CaF ₂ , MgCO ₃ , SiO ₂ , Al ₂ O ₃ , and Iron salts
(c)	SiO ₂ , Al ₂ O ₃ , CaCO ₃ , CaSO ₄ , MgCO ₃ , and Iron salts
(d)	BaSO ₄ , CaSO ₄ , CaCO ₃ , MgSO ₄ , SiO ₂ , Al ₂ O ₃ , and Iron salts
(e)	MgCO ₃ , CaCO ₃ , BaSO ₄ , CaSO ₄ , SiO ₂ , Al ₂ O ₃ , and Iron salts
(f)	CaCO ₃ , Iron salts, CaSO ₄ , and SiO ₂

3.2. Screening of Chelating Acid

As the compositions of scales are complex, the conventional mud acid is not suitable for the scales of the Hechuan gas field, as it cannot dissolve the scales such as calcium sulfate and barium sulfate, and it can also result in secondary precipitation by calcium fluoride when mud acid reacts with calcium carbonate. Therefore, it is more likely to adopt chelating acid in the Hechuan gas field. Due to its chelating ability, chelating acid can form coordination bonds with metal cations to form a soluble cyclic chelate, which breaks the dissolution balance of insoluble scales and makes them dissolve in the solution. The chelating acids are multifunctional organic weak acids containing chemical groups such as polyhydroxyl, polyamine, and polycarboxyl, etc. Fourteen kinds of self-made chelating acids were obtained by changing the ratio of each chemical group. As shown in Figure 5, there are two main mechanisms of chelating acid descaling: Firstly, the carboxyl group in chelating acid can release hydrogen ions step by step, and the hydrogen ions ionized

by the chelating acid can react with calcium carbonate to generate soluble salts, CO₂, and H₂O. With the consumption of hydrogen ions, the pH value of the system increases. When the pH rises to about 4, the isolated electrons in chelating group such as the hydroxyl group and amino group begin to form coordination bonds with metal ions such as calcium, barium, and iron, resulting in chelation, which breaks the dissolution balance of insoluble scales such as barium sulfate and calcium sulfate to make the insoluble scale gradually dissolve in the solution.

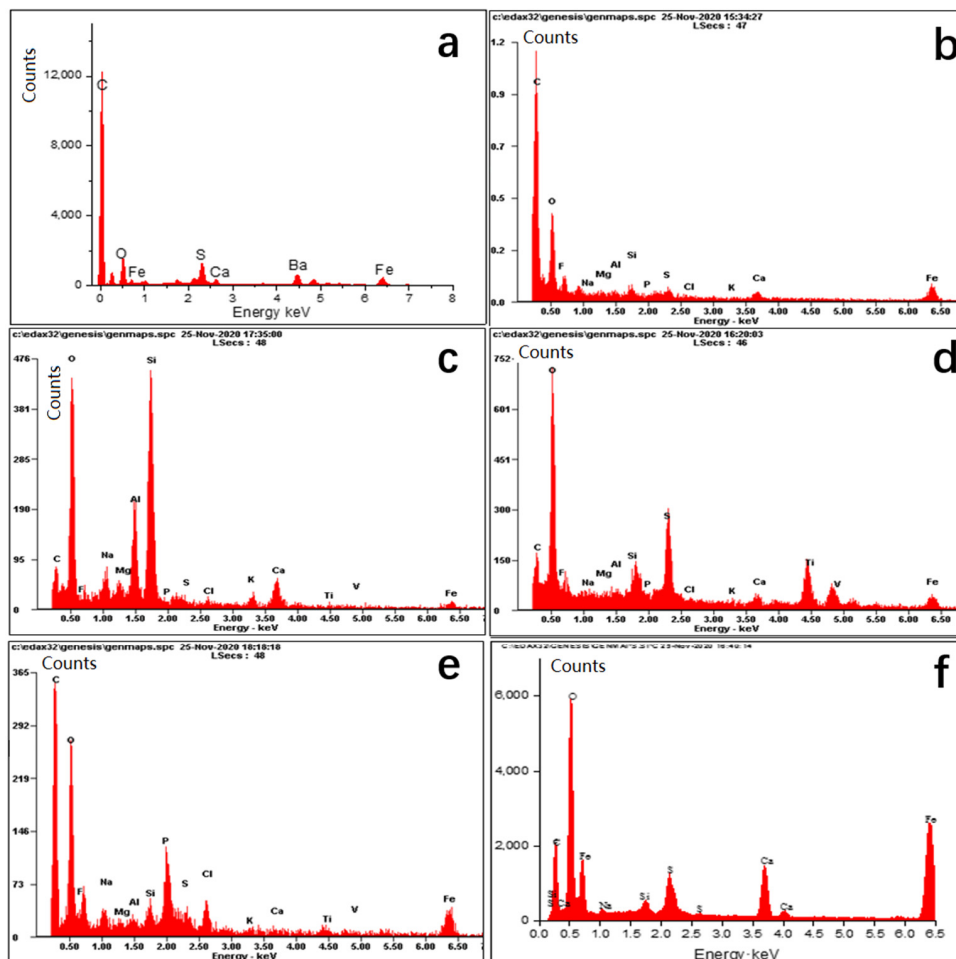


Figure 4. The EDS spectrum of scale samples of six gas wells (a–f) represents the EDS spectrum of scale sample (a), sample (b), sample (c), sample (d), sample (e), and sample (f), respectively).

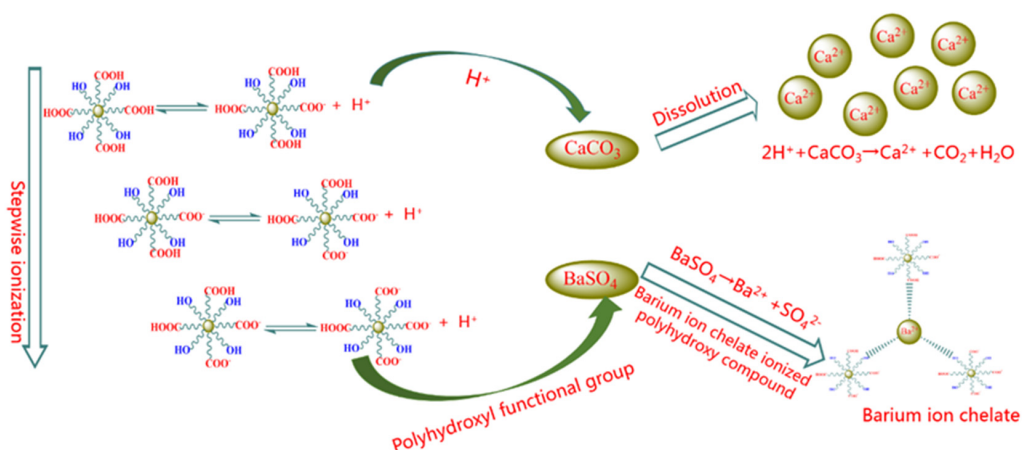


Figure 5. Schematic diagram of chelating acid descaling.

From the EDS spectra of the six scale samples, it can be seen that the proportion of insoluble scales in the scale sample (a) is higher than others that it was chosen to conduct the screening experiment of 14 chelating acids. The experimental conditions are the same in that the reaction time is set to 8 h, each acid solution volume is 20 mL with a concentration of 15%, and the scale sample is 1 g. The results are shown in Figure 6. Each chelating acid has a certain dissolution ability for scale sample (a), but the dissolution rate varies greatly, ranging from 15.5 to 77.7%, in which the dissolution effect of chelating acid AST-01 is the best with the dissolution rate of 77.7%, followed by AST-07, AST-14, and AST-13 with dissolution rates of 61.6, 61.3, and 61%, respectively. The main reason for the differences in the descaling rate for the 14 kinds of chelating acid is their ability to ionize hydrogen ions and their ability to chelate different metal ions. As different chelating acids have different chelating groups, they have different chelating and stabilizing abilities to metal ions such as calcium, magnesium, barium, and iron. Additionally, some chelating groups are sensitive to the pH value. Thus, changing the ratio of raw materials for the same scale can achieve a different descaling effect. Therefore, the chelating acid AST-01 with better performance was chosen to continue the following experiments.

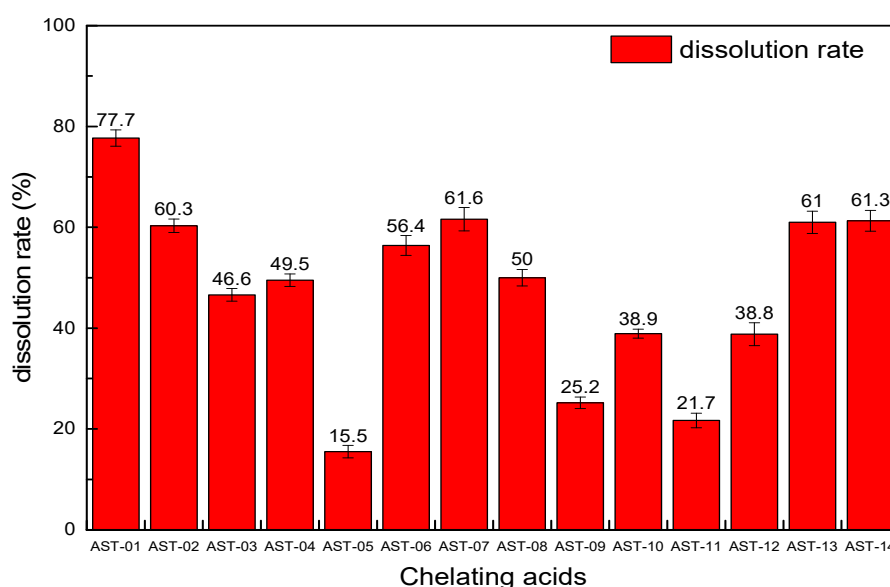


Figure 6. The dissolution rate of 14 kinds of chelating acids.

3.3. Effect of Acid Concentration on Descaling Performance of AST-01

In the above screening experiment, the acid concentration and reaction time are fixed, but they may not be the optimal value. In order to find the optimal concentration of chelating acid AST-01, the effect of scale dissolution performance of different concentrations on six scale samples was studied. The reaction time is keeping 8 h, the volume of the acid solution is still 20 mL, and the scale sample is also 1 g. The descaling rates are compared with concentrations of 5%, 10%, 15%, and 20%.

As shown in Figure 7, each line represents the scale dissolution rate at the same acid concentration for six scale samples when viewed horizontally. It can be seen that the scale dissolution rate is different due to the different compositions of each scale. There is a common feature of the curves that the dissolution rate of scale sample (c) is the lowest, but the scale sample (f) is the highest, and the other scale samples have little difference in scale dissolution rate. It can be explained according to the scale components analysis by the EDS spectrum. In Figure 4, it can be seen that the content of SiO₂ in the scale sample (c) is relatively high, which is difficult to dissolve in other acids except for hydrofluoric acid. The scale composition of the scale (f) is dominated by CaCO₃, which can easily react with an acid solution, while the content of other insoluble scales is relatively low. When viewed from the vertical in Figure 6, it can be seen that the dissolution rate of each scale sample

increases with the increase in chelating acid concentration. However, from the gap between each line, we can figure out that the average descaling rate quickly increases from 64.9 to 78.5% when the chelating acid concentration increases from 5% to 15%, and the upward trend becomes slowly when the concentration exceeds 15%. When the concentration of chelating acid is 20%, the average descaling rate of six scale samples is 82.2%. Compared with concentration of 15%, the descaling rate only increased by 3.3%, 3.2%, 3.6%, 5.4%, 4.0% and 1.6% for the scale samples (a) to (f), respectively. As the increment in chelating acid concentration, the number of groups that can chelate with metal ions also increase, which promotes the dissolution of scales. However, when the concentration increases to a certain value, the chelation effect will be weakened due to the tolerance effect [35]. Therefore, the optimal concentration of chelating acid should be between 15 and 20%, according to insoluble scale content.

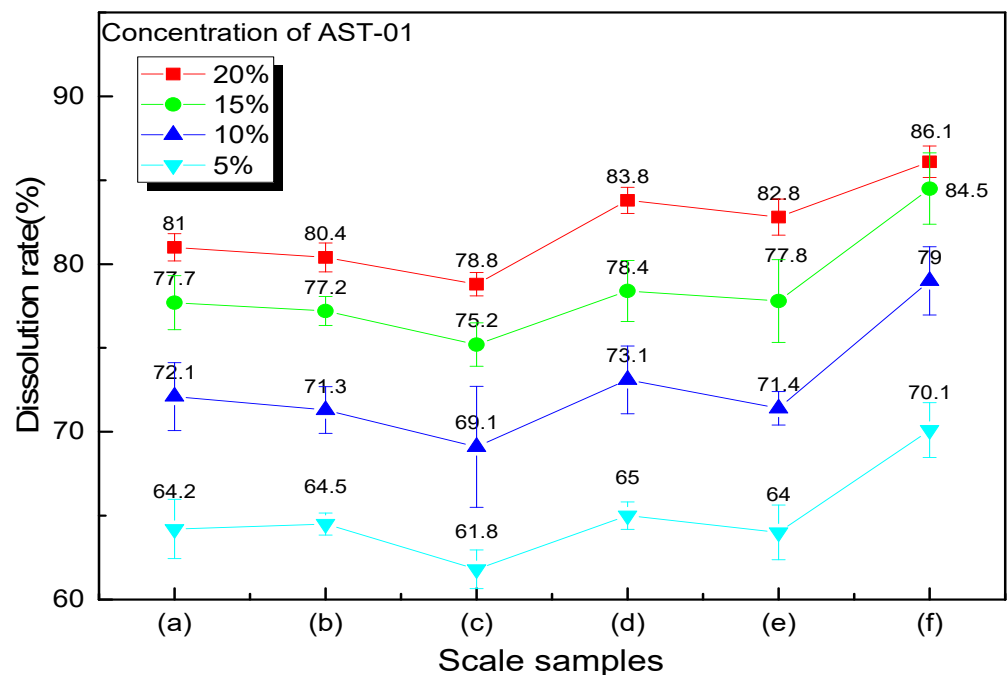


Figure 7. Descaling effect of different acid concentrations on six scale samples.

3.4. The Effect of Reaction Time on the Descaling Performance of AST-01

The chelating acid is a weak organic acid; it gradually releases hydrogen ions as the acidification reaction progresses. It has a superior retarding performance compared with conventional mud acid. In order to find the optimal reaction time of chelating acid AST-01, the effect of different reaction times on the descaling rates of the six scale samples was studied. The volume of the acid solution is 20 mL, the scale sample is 1 g, and the concentration is 15%. The descaling rate of chelating acid is compared with the reaction time of 4, 6, 8, and 10 h, respectively.

It can be seen from Table 2 that, as the reaction duration increases, the descaling rate of the six scales increases. When the reaction time is 4h, the dissolution rates of the six scale samples are all above 60%. The average descaling rate exceeds 80% when the reaction time is increased to 10 h, which is equivalent to the effect with a concentration of 20% for the reaction time of 8 h. Therefore, an appropriate increase in the reaction time is conducive to improving the descaling rate, which is determined by the chelation reaction mechanism. The contact time between the ring structure in the chelating acid and the metal ion increases, the formation of chelates can be more easily. Compared with hydrochloric acid or mud acid, chelating acid has a slower reaction speed, which allows more unreacted chelating acids to enter the reservoir to dissolve the blockage near the perforated borehole. In addition, it takes several hours for the acid to enter the formation

from the injection of the wellhead. When the acid is injected into the wellbore, the acid liquid column will increase the bottom hole pressure. As natural gas gradually flows into the wellbore under the pressure difference between formation pressure and bottom hole pressure, acid solutions will gradually enter into the reservoir. This process takes about 1~2 h in the Hechuan gas field for low formation pressure. Therefore, we recommend a shut-in time of 10–12 h to ensure that the reaction time of the chelating acid can reach 8–10 h.

Table 2. The effect of reaction duration on the descaling performance of AST-01.

Reaction Time(h)	Dissolution Rate(%)		Scale Samples			
	(a)	(b)	(c)	(d)	(e)	(f)
4	62.4	61.8	60.6	61.5	63.2	68.4
6	71.3	72.4	69.5	71.5	70.6	75.5
8	77.7	77.2	75.2	78.4	77.8	84.5
10	81.7	81.1	80.3	84.7	83.3	86.8

3.5. Optimization of the Concentration of Corrosion Inhibitor

Although the chelating acid is a weak organic acid, it is corrosive to tubing, casing, gas well Christmas trees, and ground pipelines. Thus, a certain concentration of the corrosion inhibitor needs to be added to reduce the corrosion rate of the acid. In this study, octadecyl trimethyl ammonium bromide, which is a cationic quaternary ammonium salt, is selected as the corrosion inhibitor, as it is commonly used in the acidification of oil and gas fields. The corrosion inhibition effects are studied for the corrosion inhibitor concentration is 0%, 0.5%, 0.8%, 1%, 1.5%, and 2.0% for 48 h to choose out the optimal concentration.

As shown in Table 3 and Figure 8, in this experiment, when no corrosion inhibitor is added in chelating acid AST-01, the corrosion rate is up to 193.2 g/(m²·h), and the N80 steel sheet is corroded seriously, leaving only a thin piece. With the increase in the corrosion inhibitor concentration, the corrosion rate of acid solution to the steel sheet is reduced significantly. This is as the cationic groups of the corrosion inhibitor can be adsorbed on the steel sheet to form a hydrophobic film; as the area of the adsorbed film becomes larger and denser, the electrochemical reaction on the metal surface is reduced, thus the corrosion rate is greatly reduced. When the concentration of the corrosion inhibitor reaches 1%, the corrosion rate is reduced to 1.8 g/(m²·h) and the corrosion inhibition effect is excellent, with the inhibition efficiency reaching 99.07%. Further increasing the corrosion inhibitor concentration, the corrosion rate is unchanged. However, in the actual application process, considering that the fluid accumulation in the wellbore will dilute the effective concentration of the corrosion inhibitor, it is recommended that the concentration of the corrosion inhibitor is 1.5~2%.

Table 3. The influence of corrosion inhibitor concentration on the corrosion rate.

The Concentration of Corrosion Inhibitor (%)	Corrosion Rate (g·m ⁻² ·h ⁻¹)	Corrosion Inhibition Rate (%)
0	193.2	0
0.5	78.3	59.47
0.8	37.8	80.43
1	1.8	99.07
1.5	1.5	99.22
2	1.3	99.33



Figure 8. Photographs of N80 steel sheet corrosion (left to right: 0%, 0.5%, 0.8%, 1.0%, 1.5%, and 2.0%).

3.6. Performance Evaluation of Iron Ion Stabilizer

The ESD analysis shows that there is a small number of iron scales in the scale samples. In addition, the tubing will inevitably contact the chelating acid during the descaling process. The reaction of iron salt and the corrosion of steel will produce iron ions (Fe^{2+} and Fe^{3+}). As the acidification reaction proceeds, the pH of the solution rises. When the pH value of the acid solution reaches 2.2, the Fe^{3+} ions begin to produce flocculent precipitation of $\text{Fe}(\text{OH})_3$, the dissolved trivalent iron will all precipitate to plug the reservoir and cause secondary damage when the pH value of the acid solution rises to 3.2. Therefore, it is necessary to add an iron ion stabilizer with reducing and complexing effects. The iron reducing agent can reduce Fe^{3+} to Fe^{2+} . The iron complexing agent can chelate with Fe^{2+} , which can achieve the purpose of stabilizing iron under the acidic pH value and prevent iron precipitation. The sodium erythorbate is used as the iron ion stabilizer in this experiment. The concentrations of 0.5%, 0.8%, 1.0%, 1.5%, 2.0%, and 2.5% are examined. The experimental result is shown in Table 4.

Table 4. Performance of iron ion stabilizer in different concentration.

The Concentration of Iron Ion Stabilizer (%)	Stabilizing Ability of Iron Ion (mg/mL)
0.5	34.86
0.8	44.82
1	66.66
1.5	79.01
2	89.64
2.5	93.83

With the increase concentration of the iron ion stabilizer, the ability to stabilize iron ion solution is gradually increased. The iron ion stabilization ability increases significantly when the iron ion stabilizer concentration exceeds 0.8%. The stable capacity reaches more than 80 mg/mL after the concentration exceeds 1.5%. When the concentration is 2.5%, the iron ion stabilization capacity of the solution is 93.83 mg/mL, which meets the requirements of the China National Petroleum Corporation Enterprise Standard Q/SY TZ 0082-2015. Therefore, the recommended dosage of iron ions stabilizer is 2.5%.

3.7. Optimal Concentration of Drainage Aid

After the gas well scale blockage is removed, the residual acid and dissolved scales need to be drained out of the wellbore. In order to effectively increase the degree of residual acid flow back and avoid secondary damage such as reservoir water block caused by the liquid phase, it is necessary to reduce the surface tension and interfacial tension of the acid solution. The drainage aid is prepared by combining fluorocarbon surfactants, nonionic hydrocarbon surfactants, and small molecular alcohols in a ratio of 1:60:15, and diluted by formation water to test the surface tension and interfacial tension with concentrations of 500 ppm, 1000 ppm, 2000 ppm, and 3000 ppm, respectively. The experimental results are as follows.

According to the data analysis in Figure 9, the surface tension and interfacial tension show a downward trend as the concentration of the discharge aiding agent increases. When the concentration is 500 ppm, the surface tension is 42.09 mN/m and the interfacial tension is 6.97 mN/m. When the concentration is increased to 3000 ppm, the surface tension drops to 22.64 mN/m, which is less than 30 mN/m, and the interfacial tension drops to 1.61 mN/m, which is less than 2 mN/m, meeting the requirements of “SY/T 5755-2016 Method for Performance Evaluation of Drainage Aid for Fracturing and Acidification” that the surface tension should be less than 30 mN/m, and interfacial tension should be less than 2 mN/m for a qualified drainage aid product.

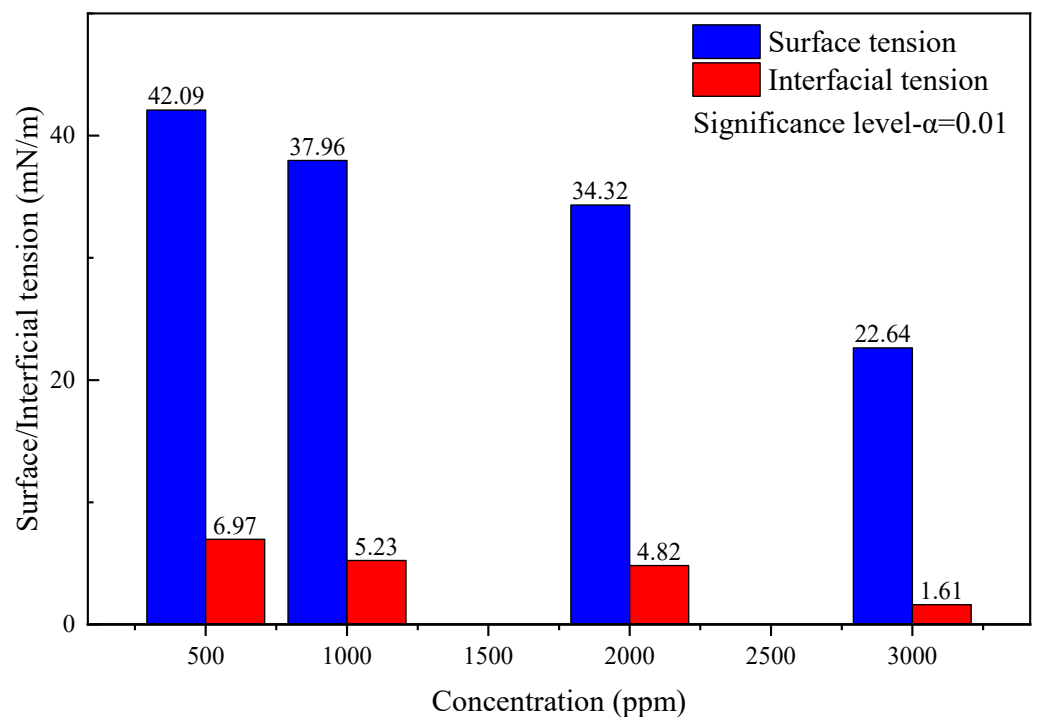


Figure 9. Surface tension and interfacial tension of discharge aiding agent.

4. Field Test of the Chelating Acid System in Hechuan Gas Field

Through the above laboratory experiments, we have obtained the chelating acid descaling system suitable for Hechuan gas field, which is 15~20% of AST-01 chelating acid + 1.5~2.0% of corrosion inhibitor + 2.5% of iron ion stabilizer + 0.3% of drainage aid. It was applied to a pilot field test in the Hechuan X1 well. In order to facilitate the analysis of the test results, a storage, electronic pressure gauge was installed to continuously monitor the shut-in tubing pressure before and after the field test. The frequency of pressure recording is to record a set of data every 3 min.

Before the plugging test, the gas well could not produce continuously due to those scales analyzed above blocking the gas flow channels such as the perforated borehole.

Generally, the tubing pressure drops to balance with the export pressure when the well is opened to produce for 4 h, resulting in a forced shut-in. The gas production is only 1000 m³. The average tubing pressure recovery rate after shut-in is 0.16 MPa/h, and the tubing pressure and casing pressure can be restored up to 9.6 MPa, but the shut-in time required is nearly 32.8 h, indicating that scale plugging has led to long-term inefficient production of this well.

As the highest shut-in wellhead pressure is only 9.6 MPa, it indicates that the formation energy of this well is not high enough. If the injection volume of the chelating acid solution is too large, it will inevitably produce a well-killing effect, and it is unable to flow back relying on the reservoir pressure. Meanwhile, due to the low production of tight reservoir gas wells, the cost of using manual assisting techniques such as gas lift has a poor economic benefit. In response to this practical problem, we proposed a low-dose and multi-round scale-removing process, which is a gradual process to dissolve the scales that blocked perforation boreholes and other parts by increasing the number of injections and flow back process, reducing the single dosage of the chelating acid solution.

The field test results are shown in Figures 10 and 11. A total of three decaling operations were carried out in this well. In the first-round scale-removing process, we designed the chelating acid system with an injection volume of 400 L. After shutting in for 10 hours, the flowback operation was implemented. When the tubing pressure dropped to 4.7 MPa, the residual acid began to flow back to the surface. The initial water sample is dark black. It can be seen that black suspended scales of small particles in the flowback fluid after leaving it for 24 h. The production of the well lasted only 1.5 h; the tubing pressure dropped to the outgoing pressure, and the water sample was clear, indicating that the residual acid had been flowing back completed and the well is shut-in. At this time, the average tubing pressure recovery rate was 0.17 MPa/h, the shut-in time needs 32.4 h for tubing and casing pressure recovering to 9.6 MPa, which is not much different from that before descaling. This shows that the amount of acid used this time is not enough to solve the scaling problem of near-well reservoirs. Therefore, we need to carry out the next round of descaling.

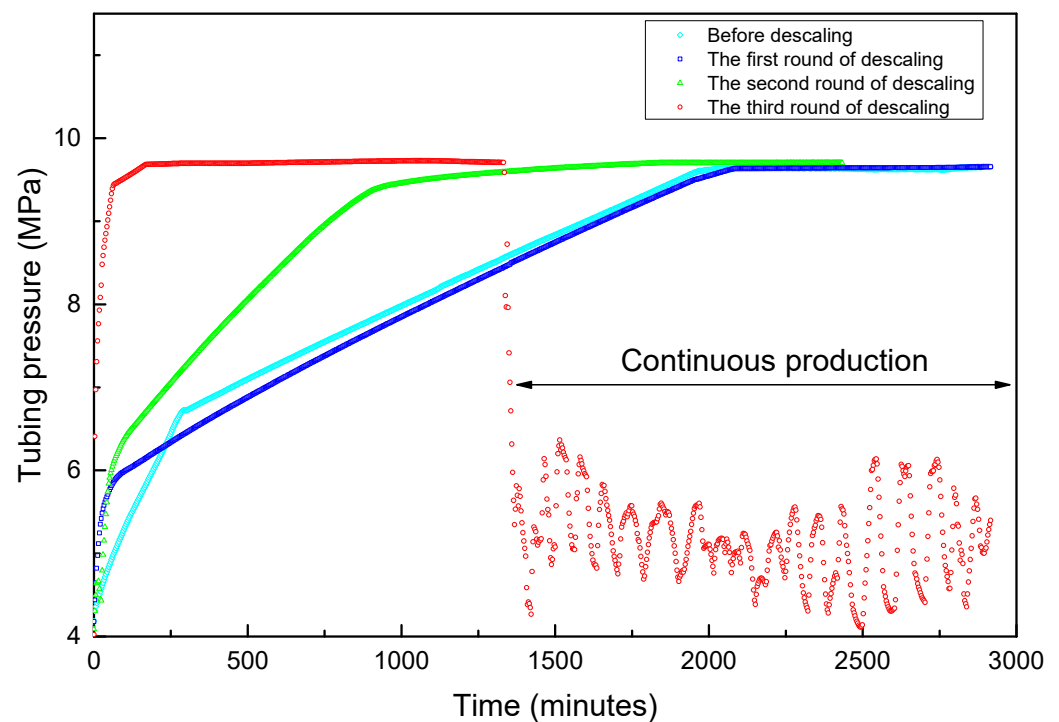


Figure 10. The real-time shut-in and production tubing pressure changes before and after descaling.

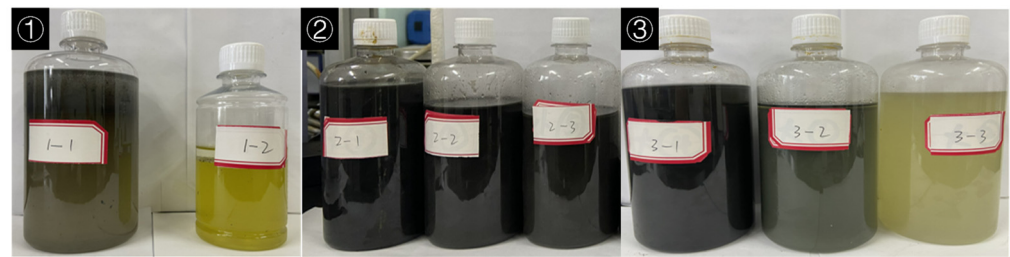


Figure 11. The water samples flowback liquids of three times descaling (1-1: The initial flowback water sample when the downhole fluid began to flow out from the wellhead for the first round descaling; 1-2: Subsequent non-scale flowback water sample for the first round descaling; 2-1: The initial flowback water sample when the downhole fluid began to flow out from the wellhead for the second round descaling; 2-2: The water sample when the volume of flowback fluid was about 300 L for the second round descaling; 2-3: The water sample when the volume of flowback fluid was about 600 L for the second round descaling; 3-1: The initial flowback water sample when the downhole fluid began to flow out from the wellhead for the third round descaling; 3-2: The water sample when the volume of flowback fluid was about 400 L for the third round descaling; 3-3: The water sample when the volume of flowback fluid was about 800 L for the third round descaling).

When the shut-in tubing pressure and casing pressure was restored to 9.6 MPa, we did the second round of descaling operation. At this time, we increased the injection volume of the chelating acid from 400 L to 600 L, and maintained the shut-in reaction time also being 10 h. The tubing pressure dropped rapidly after the well was opened. When the oil pressure dropped to 4.4 MPa, a large amount of fluid began to flow out of the ground. It was found that the color of the flowback liquid was darker than that of the first round, which was mainly due to the increase in the amount of acid solution, which increased the amount of dissolved scale. The tubing pressure dropped to the export pressure after 1 h of production. However, the shut-in tubing pressure recovery rate has been increased to 0.25 MPa/h, which can be restored to 9.6 MPa in 22.5 h. The shut-in time is reduced by 10.7 h compared with the first round. It shows that part of the scale in the near-well reservoir is gradually being dissolved, and the gas flow path has been improved, but the gas well still cannot resume continuous and stable production.

For this reason, we carried out the third round of descaling operations. We increased the amount of chelating acid to 800 L, and the shut-in reaction time remained unchanged. The fluids began to flow back when the tubing pressure dropped to 4.2 MPa after the well is opened. The initial water sample is dark black, which is close to the color of the second round of descaling, but soon later the fluid sample color became clean. The tubing pressure can still be about 0.2 MPa higher than the output pressure after 2 h of production, and the production can be continued. However, in order to test the shut-in pressure recovery rate, a shut-in operation was performed. The tubing pressure quickly recovered to 9.7 MPa at a rate of 2.4 MPa/h, and the shut-in time was only 2.3 h. The pressure recovery rate was increased by 14 times and the shut-in time was shortened by 30.5 h compared with the initial state before descaling.

Accordingly, it was believed that the scales in the near-wellbore reservoir have been completely removed. Thus, we tried to resume production and found a surprising result that the well can continuously produce with a measured gas production rate of 11,000~15,000 m³/d, the water production rate of 3~5 m³, and with the tubing pressure between 4.0~6.1 MPa. The fluctuated pressure is due to the low formation pressure and insufficient liquid-carrying capacity, resulting in a slug flow state of gas and liquid phases in the wellbore. The results obtained through the above field test once again proved that the chelating acid system developed by the laboratory experiment is reliable.

5. Conclusions

In this paper, a series of chelating acid detergents with both corrosion and chelating ability was selected, and the performance of the detergent was evaluated by laboratory experiments. The main conclusions are as follows:

- (1) Through the EDS spectroscopy analysis of scale samples from six wells, it can be inferred that the main inorganic scales in the Hechuan Gas Field are calcium carbonate, calcium sulfate, barium sulfate, formation sands, and iron salts.
- (2) From the scale dissolution rate experiment of 14 kinds of chelating acid, we screened out the AST-01 chelating acid as the main acid liquid for descaling in the Hechuan gas field. Additionally, it is determined that the best acid concentration range is 15~20%, and the reaction time is 10 h. As mentioned earlier in the article, the selection is based on the scale sample (a), the adaptability of AST-01 in the whole Hechuan area needs further study.
- (3) The concentration of additives such as the corrosion inhibitor, the iron ion stabilizer, and surfactants has also been optimized, and we have obtained the chelating acid descaling system suitable for Hechuan gas field, which is 15~20% of AST-01 chelating acid + 1.5~2.0% of corrosion inhibitor + 2.5% of iron ion stabilizer + 0.3% of drainage aid. The formula and the method presented in the article can be borrowed for the similar formation condition, which is the low-pressure sandstone gas reservoir temperature should be below 80 °C with carbonate and sulfate scales. Otherwise, the chemical compounds need to be adjusted according to the specific scale components.
- (4) The acid system has achieved very good results in the descaling field test of the Hechuan X1 well. After descaling, the shut-in oil pressure recovery rate of the gas well is 14 times that of before descaling, and the gas well resumes normal continuous production.

Author Contributions: Writing—original draft preparation, Formal analysis, Investigation, Q.L. (Qiang Li); Conceptualization and Writing—review and editing, Z.F. and Q.L. (Qingwang Liu). Resources and Visualization, G.L., J.L., W.M., N.L. and P.M. All authors have read and agreed to the published version of the manuscript.

Funding: The project is Supported by Heilongjiang Province Natural Science Foundation of “Study on flocculation of oilfield wastewater with magnetic nano-materials Fe₃O₄@SiO₂-NH₂”. Fund No.: LH2020E014.

Institutional Review Board Statement: Not applicable.

Informed Consent Statement: Not applicable.

Acknowledgments: Thanks to the laboratory support of Northeast Petroleum University and the State Key Laboratory of Oil and Gas Reservoir Development, Southwest Petroleum University.

Conflicts of Interest: The funders had no role in the design of the study; in the collection, analyses, or interpretation of data; in the writing of the manuscript, or in the decision to publish the results.

References

1. Guo, Q.; Li, X.; Zou, C.; Hu, J.; Chen, N. Predicting the distribution of the tight sandstone gas in the Hechuan play, Sichuan Basin, China. *Bull. Can. Pet. Geol.* **2012**, *60*, 186–199. [[CrossRef](#)]
2. Liqiang, S.; Yao, J.; Huang, D.; Yuan, L. Effectiveness Log Evaluation of Low Porosity and Low Permeability Sand Reservoir in Xujiahe Group of Hechuan Gas Field. *Well Logging Technol.* **2011**, *35*, 254–258. [[CrossRef](#)]
3. El-Said, M.; Ramzi, M.; Abdel-Moghny, T. Analysis of oilfield waters by ion chromatography to determine the composition of scale deposition. *Desalination* **2009**, *249*, 748–756. [[CrossRef](#)]
4. Hosny, R.; Desouky, S.E.M.; Ramzi, M.; Abdel-Moghny, T.; El-Dars, F.M.S.; Farag, A.B. Estimation of the scale deposits near wellbore via software in the presence of inhibitors. *J. Dispers. Sci. Technol.* **2009**, *30*, 204–212. [[CrossRef](#)]
5. Li, J.; Tang, M.; Ye, Z.; Chen, L.; Zhou, Y. Scale formation and control in oil and gas fields: A review. *J. Dispers. Sci. Technol.* **2016**, *38*, 661–670. [[CrossRef](#)]
6. Amjad, Z.; Hooley, J. Influence of polyelectrolytes on the crystal growth of calcium sulfate dihydrate. *J. Colloid Interface Sci.* **1986**, *111*, 496–503. [[CrossRef](#)]

7. Sun, H.; Chen, Y.; Qian, H. Progress of descaling technology in the oilfield. *Chem. Reag.* **2012**, *11*, 991–994.
8. Al-Buali, M.H.; Abulhamayel, N.; Leal, J.; Ayub, M.; Driweesh, S.; Molero, N.; Ahmed, D.; Raza, A.; La Valley, J.; Alfonzo, R.O.; et al. Recent Developments in Mechanical Descaling Operations: A Case Study from Saudi Arabia. In Proceedings of the SPE/ICoTA Coiled Tubing & Well Intervention Conference & Exhibition, Woodlands, TX, USA, 24 March 2015. [[CrossRef](#)]
9. Cheng, P.; Liu, S.; Zhang, Z.; Shuang, Z. Research and Application of High-Pressure Water Jet-Sand Blasting Descaling Technology. *Min. Res. Dev.* **2006**, *S1*, 72–75.
10. Ma, F.; Yang, N.; Liu, Y.Y. Design of high-pressure waterjet descaling nozzles testing system with LabVIEW. *Adv. Mater. Res.* **2011**, *422*, 333–337. [[CrossRef](#)]
11. Liu, Y.; Ma, F.; Xie, H.; Li, Y. Development of impact test system for waterjet descaling nozzles with LabVIEW. In Proceedings of the 2010 International Conference on Web Information Systems and Mining, Sanya, China, 23–24 October 2010; Volume 1, pp. 3–7. [[CrossRef](#)]
12. Nie, G.; Nie, R. Application of ultrasonic anti-scaling and descaling technology on heat exchange equipment. *Chlor-Alkali Ind.* **2012**, *6*, 34–38.
13. Qu, Z.; Wu, L.; An, Y.; Fang, R.; Jin, S.; Yang, J.; Liu, Y.; Wang, L.; Yang, X.; Yan, D. A descaling methodology for a water-filled pipe based on leaky guided ultrasonic waves cavitation. *Chem. Eng. Res. Des.* **2019**, *146*, 470–477. [[CrossRef](#)]
14. Yi, T. The Research Progress and Contrastive Analyses of Oilfield Descaling and Cleaning Technology. *Environ. Prot. Oil Gas Fields* **2011**, *3*, 53–55+69.
15. Son, C.-H.; Gu, S.-M.; Kim, C.-S.; Kim, G.-U. Prevention of Particulate Scale with a New winding Method in the Electronic Descaling Technology. *Trans. Korean Soc. Mech. Eng. B* **2002**, *26*, 658–665. [[CrossRef](#)]
16. Kamal, M.S.; Hussein, I.; Mahmoud, M.; Sultan, A.; Saad, M.A. Oilfield scale formation and chemical removal: A review. *J. Pet. Sci. Eng.* **2018**, *171*, 127–139. [[CrossRef](#)]
17. Gamal, H.; Elkatatny, S.; Al-Afnan, S.; Bahgat, M. Development of a unique organic acid solution for removing composite field scales. *ACS Omega* **2021**, *6*, 1205–1215. [[CrossRef](#)]
18. Chen, T.; Wang, Q.; Chang, F.; Aljeaban, N.; Alnoaimi, K. Recent Development and Remaining Challenges of Iron Sulfide Scale Mitigation in Sour-Gas Wells. *SPE Prod. Oper.* **2020**, *35*, 979–986. [[CrossRef](#)]
19. Nasr-El-Din, H.; Lynn, J.; Hashem, M.; Bitar, G.; Al-Ali, M. Lessons Learned from Descaling Wells in a Sandstone Reservoir in Saudi Arabia. In Proceedings of the International Symposium on Oilfield Scale, Aberdeen, UK, 30–31 January 2002. [[CrossRef](#)]
20. Zhou, X.; Sun, Y.; Wang, Y. Inhibition and dispersion of polyepoxysuccinate as a scale inhibitor. *J. Environ. Sci.* **2011**, *23*, S159–S161. [[CrossRef](#)]
21. Goyal, M.; Kumar, S.; Bahadur, I.; Verma, C.; Ebenso, E.E. Organic corrosion inhibitors for industrial cleaning of ferrous and non-ferrous metals in acidic solutions: A review. *J. Mol. Liq.* **2018**, *256*, 565–573. [[CrossRef](#)]
22. Zhang, G.C.; Ge, J.J.; Sun, M.Q.; Pan, B.; Mao, T.; Song, Z. Investigation of scale inhibition mechanisms based on the effect of scale inhibitor on calcium carbonate crystal forms. *Sci. China Ser. B Chem.* **2007**, *50*, 114–120. [[CrossRef](#)]
23. Klinge, L.N.; Selman, J. Chemical Cleaning of Equipment in Refineries and Petrochemical Plants. *Corrosion* **1960**, *16*, 9t–18t. [[CrossRef](#)]
24. Nasr-El-Din, H.; Hopkins, J.; Shuchart, C.; Wilkinson, T. Aluminum scaling and formation damage due to regular mud acid treatment. In Proceedings of the SPE Formation Damage Control Conference, Lafayette, LA, USA, 18–19 February 1998. [[CrossRef](#)]
25. Van Hong, L.; Mahmud, H.B. A comparative study of different acids used for sandstone acid stimulation: A literature review. In Proceedings of the IOP Conference Series: Materials Science and Engineering, Sarawak, Malaysia, 20–21 April 2017; IOP Publishing: Bristol, UK, 2017; Volume 217, p. 012018.
26. Fernando, Q.; Freiser, H. Chelating properties of β -mercaptopropionic acid. *J. Am. Chem. Soc.* **1958**, *80*, 4928–4931. [[CrossRef](#)]
27. Fushiya, S.; Sato, Y.; Nozoe, S.; Nomoto, K.; Takemoto, T.; Takagi, S.-I. Avenic acid, a new amino acid possessing an iron chelating activity. *Tetrahedron Lett.* **1980**, *21*, 3071–3072. [[CrossRef](#)]
28. Di Palma, L.; Mecozzi, R. Heavy metals mobilization from harbour sediments using EDTA and citric acid as chelating agents. *J. Hazard. Mater.* **2007**, *147*, 768–775. [[CrossRef](#)]
29. Choudry, K.; Brooke, R.C.C.; Farrar, W.; Rhodes, L. The effect of an iron chelating agent on protoporphyrin IX levels and phototoxicity in topical 5-aminolaevulinic acid photodynamic therapy. *Br. J. Dermatol.* **2003**, *149*, 124–130. [[CrossRef](#)]
30. Frenier, W.W.; Wilson, D.; Crump, D.; Jones, L. Use of highly acid-soluble chelating agents in well stimulation services. In Proceedings of the SPE Annual Technical Conference and Exhibition, Dallas, TX, USA, 1–4 October 2000. [[CrossRef](#)]
31. Wang, D.; Feng, F.; Wang, G.; Lu, Y.; Zhou, F.; Yang, G.; Gao, J. HT Carbonate Formation Acidizing Using Chelating Acid and Temperature-Control Design Method. In Proceedings of the Abu Dhabi International Petroleum Exhibition & Conference, Abu Dhabi, United Arab Emirates, 11–14 November 2019. [[CrossRef](#)]
32. Bageri, B.S.; Mahmoud, M.A.; Shawabkeh, R.A.; Al-Mutairi, S.H.; Abdulraheem, A. Toward a Complete Removal of Barite (Barium Sulfate) Scale Using Chelating Agents and Catalysts. *Arab. J. Sci. Eng.* **2017**, *42*, 1667–1674. [[CrossRef](#)]
33. Li, N.; Yang, M.; Zhang, Q.; Zhou, H.; Zhai, C.; Feng, L. A New Multiple Chelating Acid System with Low Damage and Weak Dissolution. In Proceedings of the International Petroleum Technology Conference, Beijing, China, 25–26 March 2019. [[CrossRef](#)]

-
34. Qianlong, Y.; Libiao, L.I.; Siyu, T.A.O.; Xiaobing, L.U.; Jiyun, Z.H.U. Chelate acid pulse injection and acidizing stimulation technology for immobilized injecting well string. *Pet. Drill. Tech.* **2018**, *46*, 90–94.
 35. Zhang, L.M. Study on the Synthesis of a New Type of Carboxylate Complex and its Removal of Sulfate Scale. Ph.D. Thesis, Southwest Pe-troleum University, Chengdu, China, 2015.